nature photonics

ARTICLES

PUBLISHED ONLINE: 14 FEBRUARY 2010 | DOI: 10.1038/NPHOTON.2010.6

Quantum-optical state engineering up to the two-photon level

Erwan Bimbard[1,2†], Nitin Jain[1,3†], Andrew MacRae[1] and A. I. Lvovsky[1*]

The ability to prepare arbitrary quantum states within a certain Hilbert space is the holy grail of quantum information technology. It is particularly important for light, as this is the only physical system that can communicate quantum information over long distances. We propose and experimentally verify a scheme to produce arbitrary single-mode states of a travelling light field up to the two-photon level. The desired state is remotely prepared in the signal channel of spontaneous parametric down-conversion by means of conditional measurements on the idler channel. The measurement consists of bringing the idler field into interference with two ancilla coherent states, followed by two single-photon detectors, which, in coincidence, herald the preparation event. By varying the amplitudes and phases of the ancillae, we can prepare any arbitrary superposition of zero-, one- and two-photon states.

Engineering of arbitrary quantum states in a harmonic oscillator system (such as the optical field) is complicated, because its equidistant energy levels cannot be individually accessed using classical control signals. Outside the optical domain, this challenge has been addressed in ion traps[1] and high-Q microwave cavities[2] by coupling the oscillator energy eigenstates to a two-level atomic or spin system through a sequence of simple interactions[3]. Very recently, a similar approach was used to synthesize arbitrary superpositions of Fock states of a microwave electromagnetic field inside a superconducting cavity by means of coupling to a Josephson phase qubit[4].

For travelling optical fields, quantum-state engineering (QSE) is particularly difficult because of their transient nature, which precludes the step-by-step technique of building up the required optical coherence. Therefore, a widely used approach to optical QSE involves generating a primitive quantum state of light and then manipulating it, for example, by bringing it into interference with an ancillary system. By applying appropriate measurements, the ancilla is then traced out, leading to reduction of the overall system to the desired target state, ready to be detected and characterized. The 'primitive' is commonly the state of correlated photon pairs produced in spontaneous parametric down-conversion (SPDC). Conditional photon detection on one or both channels is often used to produce the state of interest.

There exist a number of theoretical proposals for implementing optical QSE (reviewed in ref. 5), including using coherent displacements and photon subtraction operations[6,7], repeated parametric down-conversion[8] or continuous-variable post-selection[9]. Experimentally, complex entangled states of dual-rail optical qubits have been produced[10,11], albeit mostly in a post-selected manner: we do not know that the state has been prepared until it is detected and destroyed. A variety of single-mode states have been prepared without resorting to post-selection, including photon number (Fock) states $|1\rangle$ (ref. 12) and $|2\rangle$ (ref. 13), single-rail optical qubits[14–16], photon-added states[17] and the 'Schrödinger kitten' state[18,19]. However, engineering of arbitrary quantum states of light has not yet been demonstrated.

In the present work, we significantly extend the region of the optical Hilbert space within which we can engineer arbitrary states. We report, for the first time, heralded synthesis of arbitrary single-mode coherent superpositions of Fock states up to the two-photon level, with stable phase relations and a high overall efficiency. In addition to these states being of fundamental interest, they can be used for practical applications, such as optimal estimation of the loss parameter of a Gaussian bosonic channel[20].

Figure 1 shows a simplified layout of the experiment. The two-mode state produced by down-conversion can be written in the photon number basis as

$$|\Psi\rangle = \sqrt{1-\gamma^2}\left[|0_s, 0_i\rangle + \gamma|1_s, 1_i\rangle + \gamma^2|2_s, 2_i\rangle + O(\gamma^3)\right] \qquad (1)$$

where the signal and idler modes are represented by s and i, respectively, and γ is the SPDC amplitude (proportional to the pump field amplitude, effective second-order susceptibility and length of the

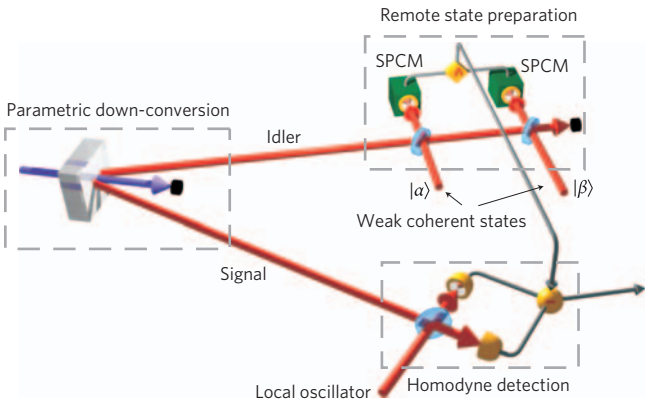

Figure 1 | Scheme to produce arbitrary quantum-optical states at the two photon level. The idler output of parametric down-conversion is mixed with two weak coherent states on beamsplitters, and the coincidence detection from the two detectors heralds the production of the expected state in the signal channel. SPCM, single-photon counting module.

[1]Institute for Quantum Information Science, University of Calgary, Calgary, Alberta, Canada T2N 1N4, [2]Département de Physique, Ecole Normale Supérieure, 24 rue Lhomond 75005 Paris, France, [3]Max Planck Institute for the Science of Light, Günther-Scharowsky-Strasse. 1, 91058 Erlangen, Germany; †These authors contributed equally to this work. *e-mail: lvov@ucalgary.ca

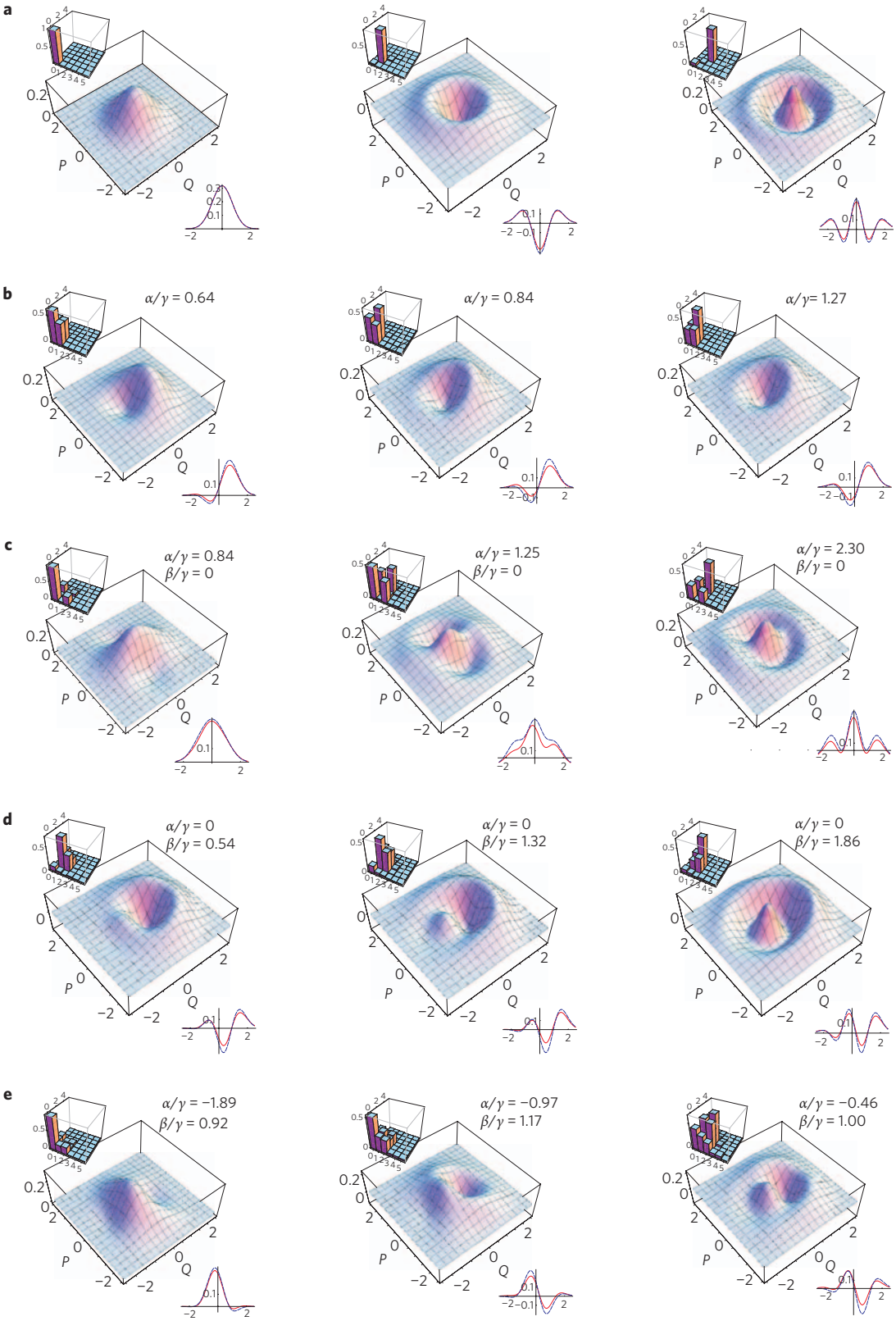

Figure 2 | Various superpositions of photon number states. In each panel, the Wigner function and the density matrix (absolute values) of the reconstructed states are displayed, as well as the cross-section of the Wigner function along the $P = 0$ plane. In the cross-sections, the solid red line shows the experimental result and the dashed blue line shows the theoretical fit (see text). All state reconstructions feature correction for 55% detection efficiency. **a**, Results for Fock states $|0\rangle$ (left), $|1\rangle$ (centre) and $|2\rangle$ (right). **b**, Superpositions of states $|0\rangle$ and $|1\rangle$. The single-photon fraction increases from left to right. **c**, Superpositions of states $|0\rangle$ and $|2\rangle$. The two-photon fraction increases from left to right. **d**, Superpositions of states $|1\rangle$ and $|2\rangle$. The two-photon fraction increases from left to right. **e**, Equal-phase superpositions of states $|0\rangle$, $|1\rangle$ and $|2\rangle$. In all plots in **e**, $a_1 \approx a_2$, and the vacuum amplitude a_0 decreases from left to right.

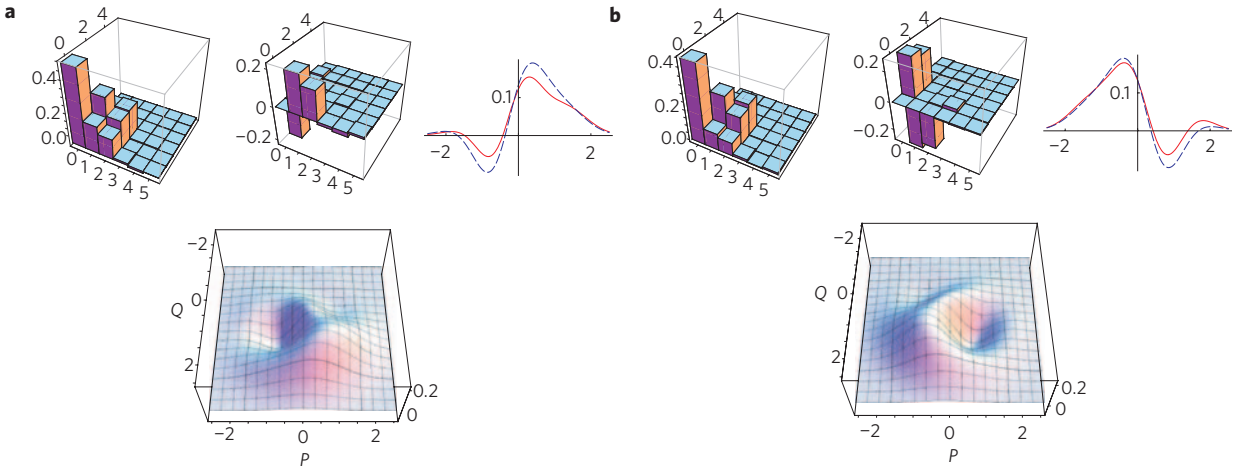

Figure 3 | Reconstructed superpositions of states $|0\rangle$, $|1\rangle$ and $|2\rangle$, corrected for detection efficiency. a,**b**, The magnitudes of a_0, a_1, and a_2 in **a** are approximately equal to those in **b**. Amplitudes a_1 and a_2 are real, whereas those of a_0 are complex conjugates of each other in **a** and **b**, so the Wigner functions appear as mirror reflections of each other. The real and imaginary components of the density matrix are shown for both states as well as the cross-section of the Wigner function along the $Q = 0$ plane (solid red line). The dashed blue lines in the cross-section plots show theoretical fits with $\alpha/\gamma = -1.14i$ and $\beta/\gamma = 1.27$ (**a**) and $\alpha/\gamma = 1.14i$ and $\beta/\gamma = 1.27$ (**b**).

nonlinear crystal). The conditional measurement is performed by mixing the idler photons with two weak ancillary coherent states of amplitudes α and β on symmetric beamsplitters, and detecting photon arrivals in two output channels. When the two detectors 'click' simultaneously, the non-locally prepared signal state is a superposition of $|0\rangle$, $|1\rangle$ and $|2\rangle$.

A qualitative explanation may be given as follows. Each of the two trigger photons can originate either from SPDC or from the ancillary states. Because SPDC emits the same number of photons into both channels, a coincidence detection event indicates that the photon number in the signal path can be, with certain probabilities, 0, 1 or 2. However, if the optical modes of the ancillary and idler fields are matched spatially and temporally, the origin of the photons detected is fundamentally indeterminable. As a result, the prepared state ρ is not simply a statistical mixture, but a coherent superposition of the first three Fock states. The coefficients of this superposition can be controlled with the amplitude and relative phase of the two ancillae.

The commercial photon detectors used in state preparation (Perkin-Elmer SPCM-AQR-14-FC, hereafter referred to as SPCM) click in response to single photons, but are unable to resolve their exact number. However, the parameters α, β and γ are on the scale of 0.1 (ref. 21), so the probability that a given click has occurred in response to two or more photons entering the detector is two orders of magnitude lower than that due to a single photon. Thus, it is safe to assume that all clicks are associated with single photons, and the contribution of $n \geq 3$ terms in the signal channel is insignificant.

In the limit of small α, β and γ, and neglecting experimental imperfections, the state prepared in the signal channel can be calculated to be (see Supplementary Information for details)

$$|\psi\rangle = a_0|0\rangle + a_1|1\rangle + a_2|2\rangle \qquad (2)$$

with

$$a_0 = -\frac{\alpha^2}{2\sqrt{2}} + \frac{\alpha\beta}{2}; \qquad a_1 = \frac{\beta\gamma}{2}; \qquad a_2 = \frac{\gamma^2}{2}$$

This equation can be interpreted easily. The zero-photon term arises from the situation when both SPCM clicks are due to the ancillae. Their interference on the two beamsplitters results in coherent fields of amplitudes $\alpha/\sqrt{2}$ and $-\alpha/2 + \beta/\sqrt{2}$ entering the SPCMs, and the value of a_0 equals the product of these amplitudes. The one-photon term arises when a photon from SPDC is registered by the first SPCM and a photon from ancilla $|\beta\rangle$ by the second, so the amplitude is $a_1 = \beta\gamma/2$. A photon originating from ancilla $|\alpha\rangle$ cannot contribute to a_1, because the Hong–Ou–Mandel interference[22] with the idler SPDC photon would prevent them from separating on the first beamsplitter. Finally, the two-photon term is due to both photons originating from the SPDC idler channel and 'choosing' those beamsplitter output paths that lead towards the two SPCMs. It is interesting that complete elimination of the $|0\rangle$ or $|1\rangle$ components from the signal state is possible simply by blocking one of the ancilla fields.

Remarkably, the entire state preparation occurs remotely, without any manipulation of the signal channel[23,24]. This is possible because the SPDC output, given by equation (1), is entangled. The low degree of entanglement associated with small γ does not restrict the range of quantum states that can be engineered; it only reduces the frequency of successful preparation events.

Our experimental set-up is detailed in the Methods. The experiment began by preparing and reconstructing the three basis Fock states in the absence of the ancillae (Fig. 2a). Subsequently, coherent superpositions of states $|0\rangle$ and $|1\rangle$, $|0\rangle$ and $|2\rangle$, and $|1\rangle$ and $|2\rangle$ were studied (Fig. 2b–d, respectively). The states in Fig. 2b were prepared by conditioning the quadrature acquisition on click events from only the first SPCM in the presence of a single ancilla field $|\alpha\rangle$. With this setting, the heralded signal state was $|\psi\rangle = \alpha|0\rangle + \gamma|1\rangle$ (ref. 14). The states in Fig. 2c,d, on the other hand, were prepared by blocking one of the weak ancilla inputs and triggering the homodyne acquisition on coincidence counts. The three examples in each subfigure contain varying weights of superposition terms, implementing gradual transition from one Fock state to another. It is interesting to note that the state in Fig. 2c, that is, the vacuum state with a small contribution of $|2\rangle$, is a good (95% fidelity) approximation of the even Schrödinger kitten state[19,25]—a superposition of two coherent states with amplitudes of ± 0.60.

Superpositions of all three Fock states are displayed in Fig. 2e. In this acquisition run, the phases of a_0, a_1 and a_2 were set to be equal by adjusting the classical interference of the two ancilla fields in the non-blocked output of the second beamsplitter to a constructive fringe. In the three states displayed, the values of β and γ were

maintained approximately the same, but the amplitude α of the first coherent state was varied. As a result, we observe a gradual transition between the vacuum state and an equal-weight coherent superposition of $|1\rangle$ and $|2\rangle$.

In all of the above examples, the zero phase reference of the reconstructed state could be chosen to make all density matrix elements real within experimental error, leading to reflection symmetry of the reconstructed Wigner functions. This is no longer the case in our two final acquisitions, aimed at demonstrating our control over the phases of a_i (Fig. 3). Here the ancillae's phases were adjusted to observe interference midway between a bright and dark fringe, on opposite fringe sides in Fig. 3a and b. This implies a phase difference of $\pm\pi/2$ between α and β. If the optical phase of the reconstructed state is chosen so that a_1 and a_2 are real, the amplitude of a_0 in Fig. 3a is a complex conjugate of that in Fig. 3b. As a result, the two Wigner functions themselves are not symmetric, but exhibit mirror symmetry with respect to each other.

To estimate the quality of our state preparation, we fitted each of the reconstructed states $\hat{\rho}$ with equation (2), aiming to maximize the fidelity $F = \langle\psi|\,\hat{\rho}\,|\psi\rangle$. The fit parameters were restricted to agree with the experimental conditions under which each data set was taken. The obtained best fit parameters are shown in Fig. 2 next to each plot. All states studied in this work exhibited at least a 76% fidelity with the fits.

To summarize, we have experimentally demonstrated the production and characterization of arbitrary superpositions of Fock states $|0\rangle$, $|1\rangle$ and $|2\rangle$ using parametric down-conversion and remote state preparation. Extension of this method to a higher photon number domain is possible, but requires additional theoretical work, as well as enhancement of the experimentally accessible photon-pair sources.

Methods

Optical set-up. We worked with 1.7-ps laser pulses at 790 nm, emitted by a mode-locked Ti:sapphire Coherent Mira 900 laser, with a repetition rate of ~76 MHz. Most of the laser energy was directed towards a LBO crystal for frequency doubling. This provided a 75 mW pump beam at 395 nm, which drove SPDC in a periodically poled $KTiOPO_4$ crystal. This crystal was phase-matched for type II down-conversion, in which the two generated modes were spatially and spectrally degenerate but had orthogonal polarizations. They were then separated spatially on a polarizing beamsplitter.

The ancilla fields also originated from the master laser. Both ancillae and the idler channel were subjected to narrowband spectral filtering (0.3 nm width) as well as spatial filtering by means of single-mode optical fibres before detection. This ensured indistinguishability of the three optical modes in the idler channel, as well as preparation of the signal state in a pure spatiotemporal mode[26].

The homodyne detector used two Hamamatsu S5972 photodiodes and featured a bandwidth of 90 MHz, which permitted time-resolved quadrature measurements at the LO pulse repetition rate[21]. Time-integrated photocurrent samples associated with each LO pulse were normalized with respect to the vacuum state, yielding quadrature data of the state measured. For each state reconstruction, 50,000 samples were typically acquired.

Phase stabilization. As is evident from equation (2), stability of the relative phase $\arg(\alpha) - \arg(\beta)$ of these states was critical for preserving coherence among different number states. The required stability was achieved by using calcite beam displacers in an interferometerically stable configuration[27] (see Supplementary Information for details). The relative phase was found to stray by less than 0.04 rad on a typical timescale of a data acquisition run (around 30 min).

The common phase of the two ancillae, as well as the phase of the SPDC pump field, were allowed to drift freely. The effect of this drift of these phases was to modify the optical phase of the signal state $|\psi\rangle$. The latter was continuously monitored in the process of homodyne detection, as we describe below.

Measuring the phase of the signal. To reconstruct the state, it is also necessary to know the phase of the signal in reference to LO for each quadrature sample. This information could be deduced by analysing time-dependent quadrature statistics, because at any given phase ϕ, the average quadrature value behaves as $\langle Q_\phi\rangle \propto \sin\phi$. However, in this experiment, the phase varied on a timescale of ~0.5 rad s^{-1}, so the coincidence-triggered data, acquired at a rate of 20–200 Hz, were insufficient for reliable phase reconstruction. Therefore, we additionally acquired the homodyne signal triggered by events from both individual single-photon detectors, which occurred at a much higher rate of 25–100 kHz. The signal states prepared by these events are phase-sensitive coherent superpositions of Fock states $|0\rangle$ and $|1\rangle$. Average quadrature values of these states over ~0.06 s periods were used to determine the LO phase at each moment in time. The phase-quadrature pairs from the acquisition were then fed to a maximum-likelihood reconstruction algorithm[28,29] to estimate the density matrix of the signal state.

Quantum efficiency. Each acquisition run began with preparation and reconstruction of single-photon Fock states, by blocking the ancilla fields ($\alpha = \beta = 0$) and triggering the quadrature acquisition by individual SPCMs. This allowed us to test the performance of our set-up and determine its overall efficiency. The latter was typically found to be between 0.52 and 0.55 due to the cumulative effect of the linear losses, SPCM dark counts, inefficient photodiodes, electronic noise and imperfect mode matching between the signal and LO[12,21]. These values are 3–6% lower than those observed in single-photon Fock state reconstruction[21]. This can be attributed to small difference between the fibres used to couple light into the SPCMs, resulting in slightly different spatial modes onto which the idler channel is projected. In applications of the state reconstruction algorithm to the Fock state superpositions, we corrected for the known inefficiency[28] using a value of $\eta = 0.55$.

Received 7 September 2009; accepted 8 January 2010; published online 14 February 2010

References

1. Ben-Kish, A. *et al.* Experimental demonstration of a technique to generate arbitrary quantum superposition states of a harmonically bound spin-1/2 particle. *Phys. Rev. Lett.* **90,** 037902 (2003).
2. Deléglise, S. *et al.* Reconstruction of non-classical cavity field states with snapshots of their decoherence. *Nature* **455,** 510–514 (2008).
3. Law, C. K. & Eberly, J. H. Arbitrary control of a quantum electromagnetic field. *Phys. Rev. Lett.* **76,** 1055–1058 (1996).
4. Hofheinz, M. *et al.* Synthesizing arbitrary quantum states in a superconducting resonator. *Nature* **459,** 546–549 (2009).
5. Dell'Anno, F., De Siena, S. & Illuminati, F. Multiphoton quantum optics and quantum state engineering. *Phys. Rep.* **428,** 53–168 (2006).
6. Dakna, M., Clausen, J., Knöll, L. & Welsch, D.-G. Generation of arbitrary quantum states of travelling fields. *Phys. Rev. A* **59,** 1658–1661 (1999).
7. Fiurášek, J., García-Patrón, R. & Cerf, N. J. Conditional generation of arbitrary single-mode quantum states of light by repeated photon subtractions. *Phys. Rev. A* **72,** 033822 (2005).
8. Clausen, J., Hansen, H., Knöll, L., Mlynek, J. & Welsch, D.-G. Conditional quantum state engineering in repeated 2-photon down conversion. *Appl. Phys. B* **72,** 43–50 (2001).
9. Lance, A. M. *et al.* Quantum-state engineering with continuous-variable post-selection. *Phys. Rev. A* **73,** 041801(R) (2006).
10. Kok, P. *et al.* Linear optical quantum computing with photonic qubits. *Rev. Mod. Phys.* **79,** 135–174 (2007).
11. White, A. G., James, D. F. V., Eberhard, P. H. & Kwiat, P. G. Nonmaximally entangled states: production, characterization, and utilization. *Phys. Rev. Lett.* **83,** 3103–3106 (1999).
12. Lvovsky, A. I. *et al.* Quantum state reconstruction of the single-photon Fock state. *Phys. Rev. Lett.* **87,** 050402 (2001).
13. Ourjoumtsev, A., Tualle-Brouri, R. & Grangier, P. Quantum homodyne tomography of a two-photon Fock state. *Phys. Rev. Lett.* **96,** 213601 (2006).
14. Resch, K. J., Lundeen, J. S. & Steinberg, A. M. Quantum state preparation and conditional coherence. *Phys. Rev. Lett.* **88,** 113601 (2002).
15. Babichev, S. A., Ries, J. & Lvovsky, A. I. Quantum scissors: teleportation of single-mode optical states by means of a nonlocal single photon. *Europhys. Lett.* **64,** 1–7 (2003).
16. Lvovsky, A. I. & Mlynek, J. Quantum-optical catalysis: generating nonclassical states of light by means of linear optics. *Phys. Rev. Lett.* **88,** 250401 (2002).
17. Zavatta, A., Viciani, S. & Bellini, M. Quantum-to-classical transition with single-photon-added coherent states of light. *Science* **306,** 660–662 (2004).
18. Ourjoumtsev, A. *et al.* Generating optical schrödinger kittens for quantum information processing. *Science* **312,** 83–86 (2006).
19. Ourjoumtsev, A., Jeong, H., Tualle-Brouri, R. & Grangier, P. Generation of optical 'Schrödinger cats' from photon number states. *Nature* **448,** 784–786 (2007).
20. Adesso, G., Dell'Anno, F., De Siena, S., Illuminati, F. & Souza, L. A. M. Optimal estimation of losses at the ultimate quantum limit with non-Gaussian states. *Phys. Rev. A* **79,** 040305(R) (2009).
21. Huisman, S. R. *et al.* Instant single-photon Fock state tomography. *Opt. Lett.* **34,** 2739–2741 (2009).
22. Hong, C. K., Ou, Z. Y. & Mandel, L. Measurement of subpicosecond time intervals between two photons by interference. *Phys. Rev. Lett.* **59,** 2044–2046 (1987).
23. Lo, H. K. Classical-communication cost in distributed quantum-information processing: a generalization of quantum-communication complexity. *Phys. Rev. A* **62,** 012313 (2000).
24. Bennett, C. H. *et al.* Remote state preparation. *Phys. Rev. Lett.* **87,** 077902 (2001).
25. Gerry, C. C. & Knight, P. L. Quantum superpositions and Schrödinger cat states in quantum optics. *Am. J. Phys.* **65,** 964–974 (1997).

26. Lvovsky, A. I. & Raymer, M. G. Continuous-variable optical quantum-state tomography. *Rev. Mod. Phys.* **81,** 299–332 (2009).
27. O'Brien, J. L., Pryde, G. J., White, A. G., Ralph, T. C. & Branning, D. Demonstration of an all-optical quantum controlled-NOT gate. *Nature* **426,** 264–267 (2003).
28. Lvovsky, A. I. Iterative maximum-likelihood reconstruction in quantum homodyne tomography. *J. Opt. B* **6,** S556–S559 (2004).
29. Řeháček, J., Hradil, Z., Knill, E. & Lvovsky, A. I. Diluted maximum-likelihood algorithm for quantum tomography. *Phys. Rev. A* **75,** 042108 (2007).

Acknowledgements

This work was supported by Natural Sciences and Engineering Research Council of Canada, iCORE, Canada Foundation for Innovation, Alberta Ingenuity Fund, Quantum*Works*, and Canadian Institute for Advanced Research. We thank S. Huisman and M. Lobino for assistance.

Author contributions

All authors contributed to the concept and design of the experiment. E.B., N.J. and A.M. implemented the experiment and acquired the data. E.B., N.J. and A.I.L. analysed the data and wrote the paper.

Additional information

The authors declare no competing financial interests. Supplementary information accompanies this paper at www.nature.com/naturephotonics. Reprints and permission information is available online at http://npg.nature.com/reprintsandpermissions/. Correspondence and requests for materials should be addressed to A.I.L.